

Selection effects on GRB spectral-energy correlations

Lara Nava^{*,†}, Giancarlo Ghirlanda[†] and Gabriele Ghisellini[†]

^{*}*Università degli Studi dell'Insubria, via Valleggio 11, Como, Italy*

[†]*Osservatorio Astronomico di Brera, via E. Bianchi 46, Merate, Lecco, Italy*

Abstract. Instrumental selection effects can act upon the estimates of the peak energy $E_{\text{peak}}^{\text{obs}}$, the fluence F and the peak flux P of GRBs. If this were the case, then the correlations involving the corresponding rest frame quantities (i.e. E_{peak} , E_{iso} and the peak luminosity L_{iso}) would be questioned. We estimated, as a function of $E_{\text{peak}}^{\text{obs}}$, the minimum peak flux necessary to trigger a GRB and the minimum fluence a burst must have to determine the value of $E_{\text{peak}}^{\text{obs}}$ by considering different instruments (BATSE, Swift, BeppoSAX). We find that the latter dominates over the former. We then study the $E_{\text{peak}}^{\text{obs}}$ -fluence (and flux) correlation in the observer plane. GRBs with redshift show well defined $E_{\text{peak}}^{\text{obs}}$ - F and $E_{\text{peak}}^{\text{obs}}$ - P correlations: in this planes the selection effects are present, but do not determine the found correlations. This is not true for Swift GRBs with redshift, for which the spectral analysis threshold does affect their distribution in the observer planes. Extending the sample to GRBs without z , we still find a significant $E_{\text{peak}}^{\text{obs}}$ - F correlation, although with a larger scatter than that defined by GRBs with redshift. We find that 6% are outliers of the Amati correlation. The $E_{\text{peak}}^{\text{obs}}$ - P correlation of GRBs with or without redshift is the same and no outlier is found among bursts without redshift.

Keywords: gamma-ray sources

PACS: 98.70.Rz

INTRODUCTION

Thanks to the discovery of the afterglow emission in long Gamma-Ray Bursts (GRBs), redshift measurements of these sources became available. The knowledge of GRB distances made possible to estimate their intrinsic properties and several correlations between prompt and afterglow properties were found. One of the most intriguing is the so called Ghirlanda correlation ([1]), linking the rest frame peak energy E_{peak} to the collimated energy E_{γ} emitted during the prompt. The possibility to use this correlation for cosmological purposes ([2]) makes it very appealing. However, the possible presence of selection effects, the lack of a physical interpretation, the difficulty in calibrating the correlation and other problems mainly related to the jet break time identification, raised objections about the validity of this correlation and/or its application in cosmology. The lack of outliers (except for GRB980425 and GRB031203, but see [3]) and the small dispersion of points around the best fit line are encouraging, but at this stage the paucity of GRBs defining this correlation (27 GRBs) prevents us from drawing any firm conclusion.

The paucity of GRBs with known E_{peak} and E_{γ} is partially due to the difficulty to estimate the jet break times. They are expected in the afterglow light curves at late times (about 1 day), when typically the light curve is not well sampled. At late times, the observations are lacking and difficult (e.g. for the presence of the host galaxy and/or a possible contamination from the underlying supernova emission) and they are not sufficient to reveal the presence of a break in the powerlaw decay behavior. The existence of other breaks and, more generally, the very complex temporal behavior discovered both in the X-ray and optical light curves, makes the situation even more confused. The different temporal decay of the X-ray and optical light curves raised the question of a different origin for these two emissions. [4] suggested that often the standard external shock model only accounts for the optical emission, whereas the X-ray has another (internal) origin. According to this interpretation, [5] caution about the identification of jet break times, pointing out that they should be identified in the optical light curves, at late times. According to the modeling of [6], these breaks could also be chromatic.

When the jet break time is not available, we can only estimate the isotropic equivalent energy E_{iso} , i.e. the energy emitted during the prompt by assuming an isotropic emission geometry. The quantity E_{iso} still shows a correlation with E_{peak} (the so called Amati correlation, [7]), in the form $E_{\text{peak}} \propto E_{\text{iso}}^{0.5}$. This correlation, found before the Ghirlanda one, displays a larger scatter and a different slope. Assuming the validity of the E_{peak} - E_{γ} correlation, the presence of this large scatter in the Amati correlation can be easily explained, assuming that a wide range of jet opening angles θ_j can

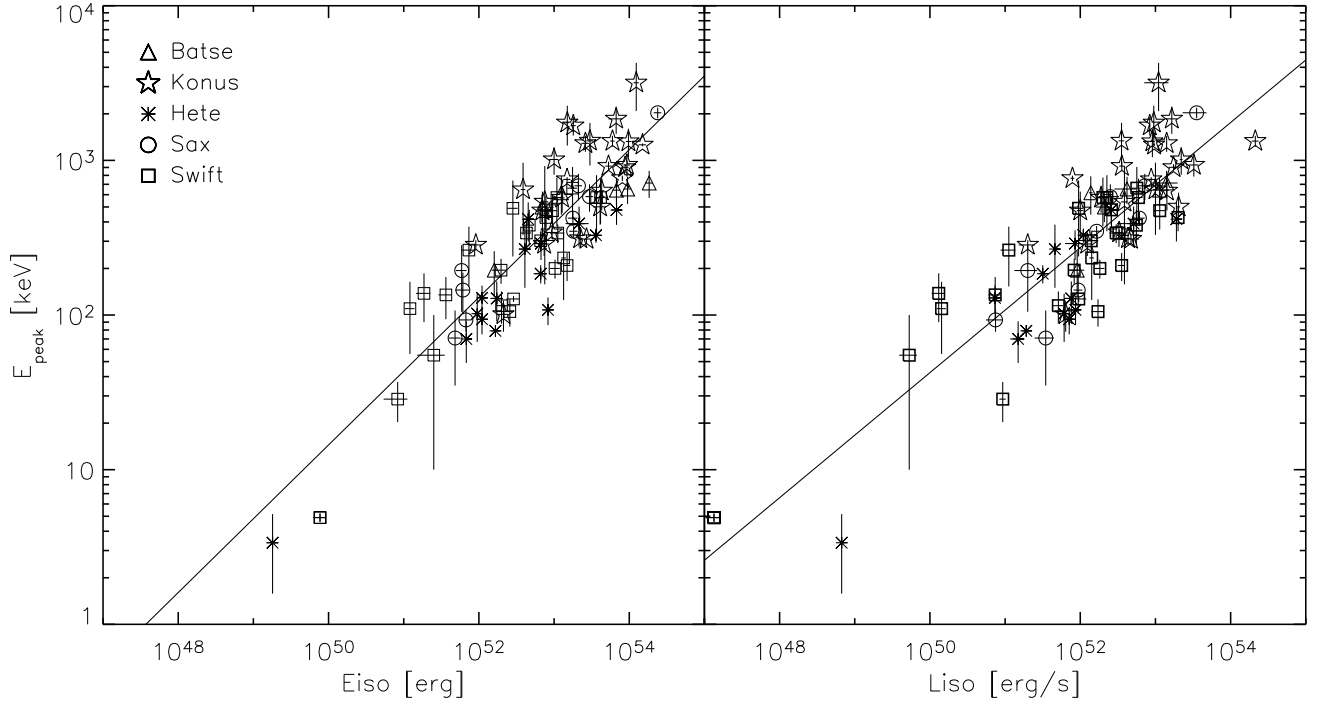


FIGURE 1. $E_{\text{peak}}-E_{\text{iso}}$ and $E_{\text{peak}}-L_{\text{iso}}$ correlations for 83 GRBs with measured redshift and spectral parameters. The slopes obtained from the fit with a power law model are respectively 0.48 ± 0.03 and 0.40 ± 0.03 . Modeling the scatter distributions with a gaussian function we found respectively $\sigma = 0.23$ and $\sigma = 0.28$.

correspond to bursts with same E_{γ} (and therefore, for the $E_{\text{peak}}-E_{\gamma}$ correlation, same E_{peak}). This range of θ_j values reflects into a range of E_{iso} values, for the same given E_{peak} .

Independently from its origin, the large dispersion of the Amati correlation makes it unsuitable for the cosmological applications, unless systematics, unknown, extra scatter terms are introduced.

Despite these problems, the Amati correlation appears robust. Although the number of GRBs with known E_{peak} and E_{iso} is reasonably large (83 objects in [8]), only two of them do not obey the Amati correlation. Note that these two outliers are very peculiar GRBs (see [3]). Moreover, the validity of the correlation has been extended to XRFs and now spans five orders of magnitudes in E_{iso} , from XRFs to very bright GRBs. This behavior calls for a theoretical explanation. Some works ([9], [10], [11]) suggest that its existence is due to the presence of selection effects. To check this possibility it is necessary to perform a systematic and accurate study of all the possible selection effects, to better understand if and how they affect the correlation.

Another correlation involving similar quantities is between E_{peak} and L_{iso} (Yonetoku correlation). [12] found this correlation defining L_{iso} as the luminosity emitted at the peak of the light curve. In its original form, this correlation appeared slightly tighter than the Amati one, but with a similar slope. We will also study selection effects on this correlation. Fig. 1 shows both the $E_{\text{peak}}-E_{\text{iso}}$ and the $E_{\text{peak}}-L_{\text{iso}}$ correlations updated to April 2008 ([8]). The analysis performed on this sample (83 GRBs) shows that the $E_{\text{peak}}-L_{\text{iso}}$ correlation displays a larger scatter than the $E_{\text{peak}}-E_{\text{iso}}$ correlation and therefore the latter seems to be more fundamental (see [8] for details).

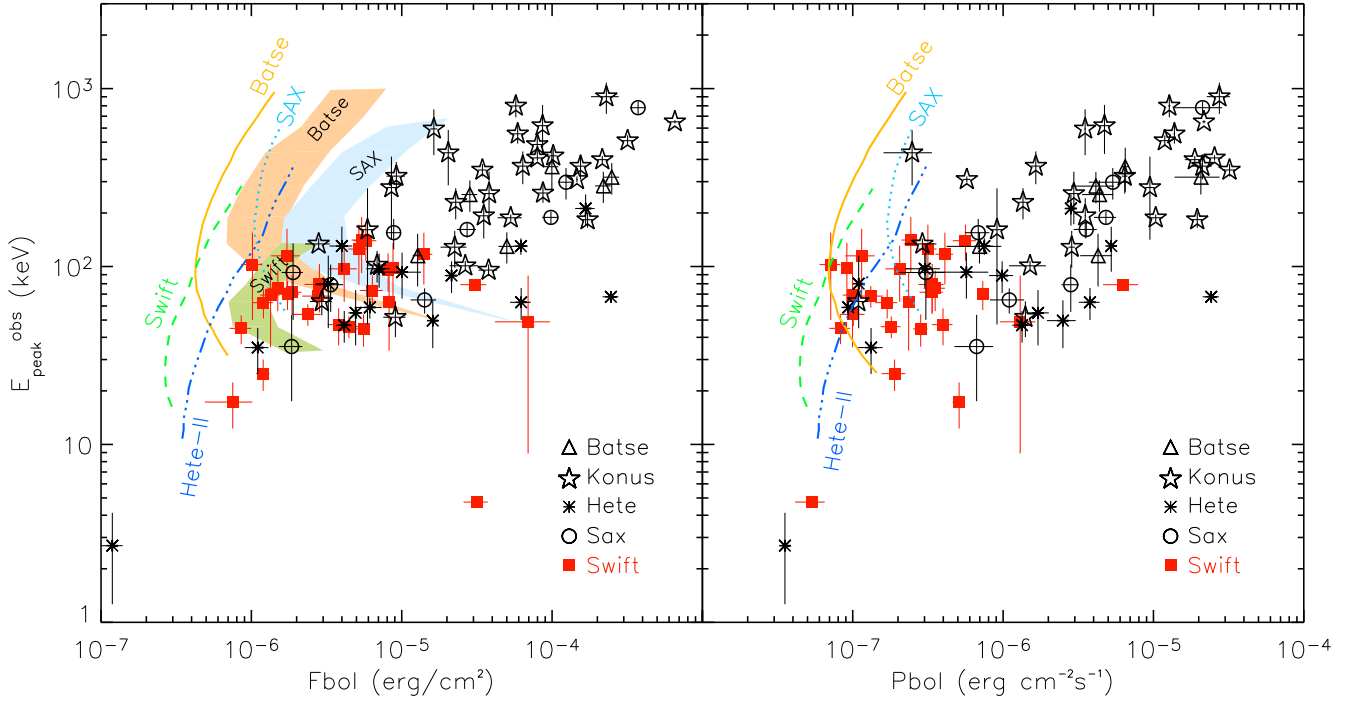


FIGURE 2. Distributions of 83 GRBs with known redshifts in the $E_{\text{peak}}^{\text{obs}}$ -Fluence and $E_{\text{peak}}^{\text{obs}}$ -Peak flux planes. In both cases, they define a correlation in the observational planes. Shaded regions in the right panel show the ST (see text) for different instruments: for each instruments it is possible to perform a reliable spectral analysis only for bursts that lie on the right side of these regions. In both the panels, the curves show the TT (see text) for different instruments: only bursts at the right side can be detected.

INSTRUMENTAL SELECTION EFFECTS

We are interested in studying the rest frame correlations $E_{\text{peak}}-E_{\text{iso}}$ and $E_{\text{peak}}-L_{\text{iso}}$. However, instrumental selection effects act on the corresponding observational quantities: $E_{\text{peak}}^{\text{obs}}$, Fluence (F) and Peak-Flux (P). In Fig. 2 we report the sample of 83 GRBs with known redshift plotted in the observational planes $E_{\text{peak}}^{\text{obs}}$ -F and $E_{\text{peak}}^{\text{obs}}$ -P. Also in these planes, this sample of GRBs defines a correlation.

Instrumental limits are obviously present. For example, very faint bursts can not be detected by a given instrument if they are below its trigger threshold. It is possible that the correlation is completely due to selection effects that make accessible only a small part (a stripe) of the whole observational plane. However, note that the region at the right side of the $E_{\text{peak}}^{\text{obs}}$ -F ($E_{\text{peak}}^{\text{obs}}$ -P) correlation can not be affected by instrumental selection effects, since bursts in this region would have an intermediate/low E_{peak} (easily measurable by instruments) and a high fluence (peak flux). The lack of bursts in this region strongly suggests that bursts with these characteristics do not exist or they are very few. On the left side of the two correlations we can face with two different situations: the unavoidable selection effects acting in these regions can i) lie far from the position of observed GRBs (in this case the observed distribution of points is not determined by selection effects) or ii) lie very close to points, indicating that they determine the shape of GRBs distribution in this part of plane. To discriminate between these two cases, we need to quantify the selection effects.

We identified the two most probable instrumental selection effects that can affect the sample:

- the trigger threshold (TT): it is very complex to quantify what characteristic a burst must have to be detected by a given instrument. To a first approximation, we can affirm that it must have a minimum photon peak flux. This translate into a minimum energy flux, whose value depends on the spectral properties of the burst (especially $E_{\text{peak}}^{\text{obs}}$). For several instrument [13] derive the curves of minimum peak flux as a function of $E_{\text{peak}}^{\text{obs}}$. We plot these curves in the $E_{\text{peak}}^{\text{obs}}$ -P plane, after accounting for the bolometric correction. Considering a typical conversion factor between fluence and peak flux of ~ 6 ([14]), we plot these curves also in the $E_{\text{peak}}^{\text{obs}}$ -Fluence plane.

- the spectral analysis threshold (ST): we need a minimum fluence to perform a reliable spectral analysis and determine $E_{\text{peak}}^{\text{obs}}$ and the spectral shape. [14] consider this problem by accounting for the detector response and the typical background of each instrument. For each $E_{\text{peak}}^{\text{obs}}$ they determine this limiting fluence and obtain a curve in the $E_{\text{peak}}^{\text{obs}}$ -F plane. Its position depends on the burst duration. In Fig. 2 (left panel) we show the ST as a shaded region: the left (right) edge represents the curve obtained for bursts lasting 5 (20) seconds.

Comparing the position of points in Fig. 2 detected by a given instrument with the corresponding threshold curves we can draw several conclusions. In the $E_{\text{peak}}^{\text{obs}}$ -F plane the ST represents a more important selection effect compared to the TT. Swift bursts (filled squares) are strongly affected by the corresponding ST limiting curves. Note that for Swift bursts we mean bursts whose $E_{\text{peak}}^{\text{obs}}$ has been determined from the modeling of the BAT data. However, this instrument can only measure $E_{\text{peak}}^{\text{obs}}$ within the range 15-150 keV. Consequently, the Swift sample is distributed in a very narrow range in $E_{\text{peak}}^{\text{obs}}$, smaller than the scatter of the $E_{\text{peak}}^{\text{obs}}$ -F correlation as defined by all the pre-Swift bursts. For this reason, we caution about the use of Swift bursts to test the existence of this correlation.

Our results also show that the pre-Swift GRB sample, containing a fraction of bursts detected by BeppoSAX and BATSE, is not affected by the corresponding limiting curves. This is particularly evident for high $E_{\text{peak}}^{\text{obs}}$, where the limiting curves lie far from the points. A similar conclusion can be drawn for the $E_{\text{peak}}^{\text{obs}}$ -P correlation (right panel). Points are slightly affected by the corresponding TT in the region at low peak flux, but the behavior according to which higher peak fluxes correspond to higher $E_{\text{peak}}^{\text{obs}}$ is not due to the threshold.

In both planes however, the lack of bursts (with known redshift) with intermediate/large $E_{\text{peak}}^{\text{obs}}$ and small fluence or peak flux (i.e. between the present sample of GRBs and the limiting curves) could be due to the additional presence of a still-not-understood selection effect, for example linked to the redshift determination. The first step to investigate this possibility is to search if there exist GRBs which populate the region on the left-hand side of the $E_{\text{peak}}^{\text{obs}}$ -F and $E_{\text{peak}}^{\text{obs}}$ -P correlations. This issue can be solved by including, in both plots, all the bursts with measured spectral properties, without the request of knowing their redshifts.

GRBS WITHOUT REDSHIFT MEASUREMENT

In this section we study the very same issue tackled in the previous one, but considering all bursts found in literature with measured $E_{\text{peak}}^{\text{obs}}$ and spectral properties. For this reasons, we considered Hete-II bursts ([15]), Swift bursts ([9]) and the sample of bright BATSE bursts ([16]). Moreover, we collected the preliminary results arising from the analysis of the Konus-Wind spectra as reported in the GCN circulars (29 GRBs). To extend the sample of BATSE bursts to lower fluences we performed the spectral analysis of 100 BATSE bursts down to 10^{-6} erg/cm² (see [8] for details).

Fig. 3 (left panel) reports the distribution of all these bursts in the $E_{\text{peak}}^{\text{obs}}$ -F plane. Different symbols refers to different instruments. We note that the entire sample of GRBs without redshift seems to occupy a larger region with respect to GRBs with redshift (filled squares) studied in the previous section. In particular, they enlarge the distribution toward the ST curves. However, moving towards lower fluence values their density decreases (see [8] for more details). In other words, points do not uniformly fill all the accessible plane, but are concentrated along a strip whose slope and position is not determined by the considered selection effects. Therefore, the existence of the Amati correlation must have a physical origin. However, the dispersion of the whole sample of GRBs is larger then that defined only by GRBs with redshift. This suggests that, if we were able to measure the distance of all GRBs in Fig. 3, we should find an Amati correlation with different properties, such as a larger scatter and, likely, a different slope. The grey region in the top left corner of the $E_{\text{peak}}^{\text{obs}}$ -F plane (see Fig. 3) shows the region where bursts are outliers of the Amati correlation (as defined by the sample of 83 GRBs with redshift). This means that GRBs that lie in this region can not be consistent with the correlation for any redshift. For 'consistent' we mean the burst must fall within the 3σ scatter of the correlation. We found that the 6% of the sample is not consistent with the Amati correlation.

The right panel of Fig. 3 refers to the $E_{\text{peak}}^{\text{obs}}$ -Peak flux plane. Also in this case it is evident the presence of a correlation, i.e. of a distribution of points that preferentially lie along a strip. This behavior cannot be explained in terms of selection effects, since the shape and the position of the TT curves cannot account for the observed distribution of points. The difference with respect to the case of the $E_{\text{peak}}^{\text{obs}}$ -F correlation is that, here, the distribution of points without redshift seems to better agree with that of GRBs with redshift. This suggests that in the future, when a larger sample of GRBs with redshift will be available, the properties of the Yonetoku correlation (slope and scatter) will resemble those of the present correlation. Also in this plane we have estimated the regions of outliers and we found only one burst which cannot be consistent with the correlation.

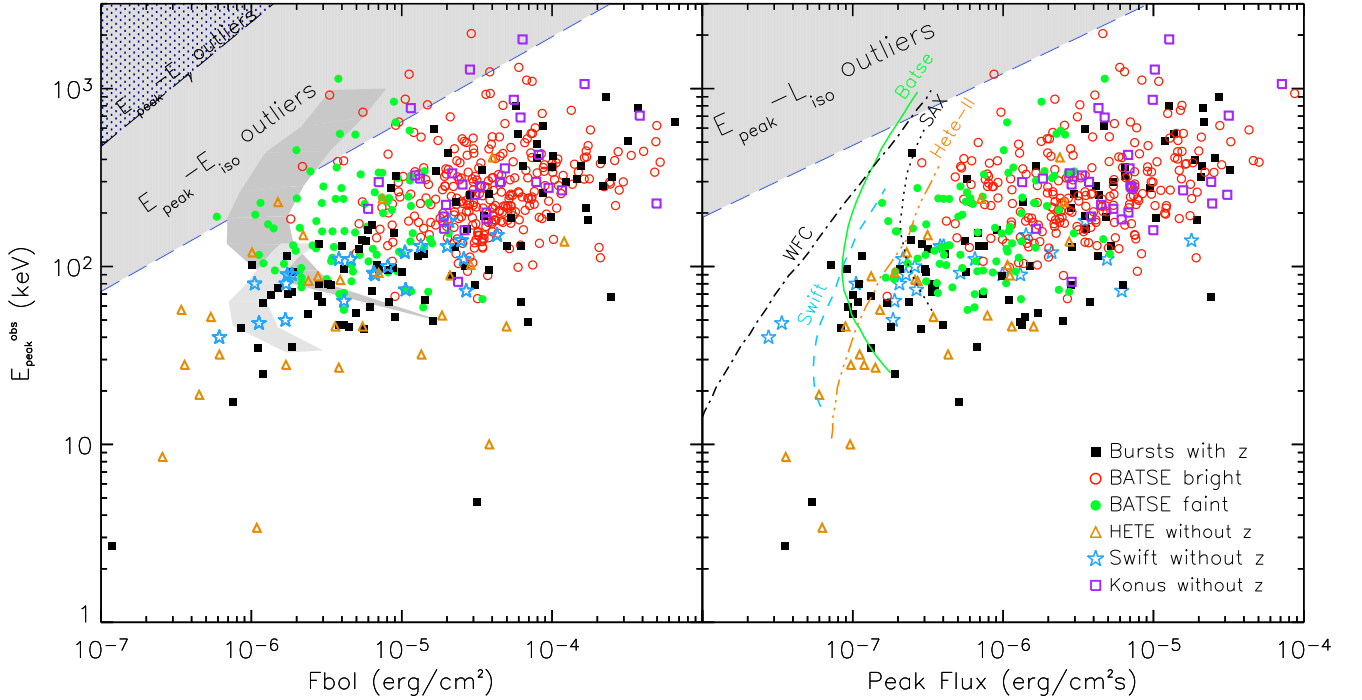


FIGURE 3. Left panel: bursts with (filled squares) and without (other symbols) known redshift in the $E_{\text{peak}}^{\text{obs}}$ -Fluence plane. Shaded curves represent the ST curves for BATSE and Swift/BAT instruments (see Fig. 2). Shaded regions in the top left corner show which bursts can not be consistent with the 3σ scatter of the Amati relation defined in the rest frame plane by GRBs with redshift. Right panel: $E_{\text{peak}}^{\text{obs}}$ -Peak flux plane. Curves show for several instrument the TT, i.e. the minimum peak flux required to detect the burst. In this case only one burst fall in the region of outliers.

CONCLUSIONS

To study the role of possible instrumental selection effects on the Amati and Yonetoku relation, we have considered the distribution of GRBs with and without known redshift in the observational $E_{\text{peak}}^{\text{obs}}$ -Fluence and $E_{\text{peak}}^{\text{obs}}$ -Peak flux planes. Following the analysis performed by [14], we refer to two different instrumental biases: the trigger threshold (TT, the minimum peak flux required to trigger a burst) and the spectral analysis threshold (ST, the minimum fluence needed to constrain the GRB spectral properties). These curves depend on $E_{\text{peak}}^{\text{obs}}$ and define what part of the observational planes is accessible: only bursts at the right side of both the curves can be plotted in these planes, the other bursts have no sufficient flux to be detected or no sufficient fluence to recover $E_{\text{peak}}^{\text{obs}}$ and the spectral shape from the spectral analysis. We note that in both the observational planes GRBs are not spread in the region free from instrumental selection effects, but define a correlation. Note that the shape of this concentration of points is not determined by the considered thresholds. Their only effect is to cut the part of the correlations corresponding to the smallest $E_{\text{peak}}^{\text{obs}}$ and Fluences/Peak fluxes. From the comparison between bursts with and without redshift we can conclude that there exists an $E_{\text{peak}}-E_{\text{iso}}$ correlation not determined by selection effects, even if its slope and scatter may be different from what we know now. On the other hand, we suggest that, once a large number of bursts with redshift will be available, the Yonetoku correlation will preserve more or less the present scatter and slope.

Another hint in favor of the relevance of the $E_{\text{peak}}-L_{\text{iso}}$ correlation comes from short bursts. A detailed analysis of a large sample of short bursts performed by [17] shows that they have a similar $E_{\text{peak}}^{\text{obs}}$ and Peak flux of long GRBs and, indeed, they populate the same region in the $E_{\text{peak}}^{\text{obs}}$ -Peak flux plane. This suggests they can be consistent with the same $E_{\text{peak}}-L_{\text{iso}}$ correlation defined by long GRBs (this is also confirmed by the few short bursts for which we know the redshift). Short GRBs, instead, are inconsistent with the distribution of long GRBs in the $E_{\text{peak}}^{\text{obs}}$ -Fluence plane, since, for the very same $E_{\text{peak}}^{\text{obs}}$ they have a smaller fluence. This implies that the majority of short GRBs are outliers of the $E_{\text{peak}}-E_{\text{iso}}$ correlation defined by long bursts.

REFERENCES

1. G. Ghirlanda, G. Ghisellini, and D. Lazzati, 2004, *ApJ*, 616, 331
2. G. Ghirlanda et al., 2004, *ApJ*, 613, 13
3. G. Ghisellini et al., 2006, *MNRAS*, 372, 1699
4. G. Ghisellini et al., 2007, *ApJ*, 658L, 75
5. G. Ghirlanda et al., 2007, *A&A*, 466, 127
6. G. Ghisellini et al., 2009, *MNRAS*, 393, 253
7. L. Amati et al., 2002, *A&A*, 390, 81
8. L. Nava et al., 2008, *MNRAS*, 391, 639
9. N. Butler et al., 2007, *ApJ*, 671, 656
10. E. Nakar and T. Piran, 2005, *MNRAS*, 360, 73
11. D. Band and R. Preece, 2005, *ApJ*, 627, 319
12. D. Yonetoku et al., 2004, *ApJ*, 609, 935
13. D. Band, 2003, *ApJ*, 588, 945
14. G. Ghirlanda et al., 2008, *MNRAS*, 387, 319
15. T. Sakamoto et al., *ApJ*, 629, 311
16. Y. Kaneko et al., 2006, *ApJS*, 166, 298
17. G. Ghirlanda et al., 2009, accepted by *A&A*